Thermal Stresses Around Penetration Sleeve in Concrete Containment Vessels

G. Yoneda
Takenaka Komuten Co., Ltd., Office of Nuclear Engineering, 21-1, Ginza 8-chome, Chuo-ku, Tokyo 104, Japan
M. Ueda, K. Okada
Takenaka Komuten Co., Ltd., Takenaka Technical Research Laboratory, 5-14, Minamisuna 2-chome, Koto-ku, Tokyo 136, Japan

Abstract

Generally, there are many pipe penetrations in a reinforced or prestressed concrete containment vessel, and the steel sleeves around the penetrations are anchored in the concrete. When these sleeves are subjected to high atmospheric temperature during loss of coolant accident (LOCA), their thermal expansion in the radial direction is confined by the surrounding concrete. Therefore, compressive force in the radial direction and tensile force in the circumferential direction react around the circular penetrations.

Thermal stresses, however, decrease due to cracking and/or creeping of concrete, and many studies have been reported on this. But in-plane thermal stresses around pipe penetrations have not yet been made clear. Therefore, experimental and analytical studies were carried out in order to obtain fundamental data on thermal stresses around pipe penetrations.

1. Introduction

Reinforced or prestressed concrete containment vessels (CCV) of a nuclear power plant are subjected to temperatures of 50 to 60°C at normal operating state and about 150°C at LOCA. So, thermal load greatly affects the structural design of a CCV. Around a pipe penetration, the thermal expansion of a penetration sleeve causes a compressive force in the radial direction and a tensile force in the circumferential direction. We herein call these thermal stresses "sleeve thrusts". Please note that the main steam penetration sleeve is made very thick in order to withstand the loads of pipe ruptures. Thus the sleeve thrust around it is very large and much reinforcement is required if the elastic theory is adopted. It, however, may be reduced because thermal stresses decrease in accordance with the stiffness reduction caused by the cracking of concrete. In this study the sleeve thrust was investigated through experiments and by non-linear finite element analysis.

Test specimens used were circular reinforced concrete plates with a center hole and a steel sleeve was placed around it. The stresses, cracking and deformation were observed by heating the sleeve up to 150°C. The test results were then simulated by the non-linear finite element method (FEM). In addition, several parametric studies by the same non-linear FEM were carried out in order to examine the general behaviour of the sleeve thrust.

The parameters were sleeve thickness, reinforcement ratio and the stress condition of concrete (compressive or tensile state). The mechanism for the sleeve thrust were satisfactorily determined through these experiments and FE-analyses. The results have provided practical guides for rational section design method for the sleeve thrust.

2. Experimental Study

2.1 Test Specimen: The experiments consisted of two types. One was a pressure test to examine the elasto-plastic property of concrete around a circular penetration and the other was a sleeve heating test to examine the sleeve thrust force. Four specimens of circular reinforced concrete plates which represented the penetration area in a shell wall of a CCV were provided. As illustrated in Fig. 1, the test specimens were 180 cm in diameter, and 20 cm in thickness with a center hole 36 cm in diameter. The experimental parameter was the reinforcement ratio. Deformed bars, 16 mm in diameter, were arranged at 22.5° spacings in the radial direction and two kinds of deformed bars, 16 mm and 22 mm, were arranged at 9 cm spacings in the circumferential direction, respectively. The reinforcement ratio in the circumferential direction was 1.16% and 2.11%. The test parameters and material properties are summarized in Table 1 and Table 2.

2.2 Test Procedure: In the pressure test, the radial force equivalent to the sleeve thrust was applied onto the inside surface of the center hole. In the heating test the steel sleeve was heated up to 150°C, and kept a constant 150°C during the test period. The surface of the specimen was covered with an asbestos thermo-insulator to prevent heat issue. In order to simulate the stress state at LOCA, when increased inside pressure causes membrane tensile force on the shell wall of a CCV, the test specimen was pulled by PC rods from the outside in both tests. PC rods were attached to radial reinforcements with a coupler and pulled by sixteen center-hole-jacks which were supported through a reaction ring. The test apparatus and loading condition are shown in Fig. 2 and Fig. 3, respectively.

2.3 Test Results

Pressure Test: Cracking was observed at 20 ~ 30 kgf/cm^2 pressure level, and developed in radial directions. As shown in Fig. 4, the spacing of cracks at the ultimate state was about 22.5° in both C16 and C22 specimens. The relationships between pressure load and radial displacement are shown in Fig. 5, and the stress distributions of circumferential reinforcements are shown in Fig. 6. Displacement and reinforcement stress decreased at the outside of the specimen.

Heating Test: Fig. 7 shows the temperature distribution of the H16 specimen at each instance of loading. Sleeve temperature was raised to 150°C in twenty-five minutes. Heat was conducted to the concrete through the sleeve, but during the test period temperature was almost constant at more than twice the distance of the opening radius. The same temperature distribution was observed in the H22 specimen.

As in the pressure test, radial cracks were observed at 22.5° spacings. Three dimensional relationship among crack width at a distance of 3 cm from the edge of the center hole, sleeve temperature and time under thermal load is shown in Fig. 8. In the early heating stage crack widths became wider in accordance with the rising temperature and a maximum crack width reached 0.22 mm in H16 and 0.17 mm in H22, respectively. Thereafter, as heat was conducted to the concrete, the crack widths near the center hole tended to decrease due to the thermal expansion of concrete.

Fig. 9 shows the stress of circumferential reinforcements. In the early heating stage re-bar stress became higher in accordance with the rising temperature. However, at higher than 50°C the re-bar stress in the vicinity of the center hole didn't increase as much as that of the outside due to the stress re-distribution by the cracking of the specimen and/or thermal expansion of concrete. At last, as shown in Fig. 10, the most inside re-bar stress became compressive in the heating test.

2.4 Discussion of Test Results: According to the elastic theory, pressure load Ps caused by the thermal expansion of the sleeve is calculated by equation (1).[1]

$$Ps = \frac{Es\ (\alpha s\ Ts - \alpha c\ Tc)}{\frac{Es}{Ec}\left(\frac{b^2 + a^2}{b^2 - a^2} + \nu c\right) + \frac{a}{t}} \qquad (1)$$

where Ts: sleeve temperature
Es, Ec: elastic modulus of sleeve and concrete
αs, αc: linear thermal expansion coefficient of sleeve and concrete
Tc: average temperature of concrete
νc: Poisson's ratio of concrete
t: sleeve thickness
a: radius of the sleeve
b: outer radius of concrete

The sleeve thrust calculated by equation (1) and the measured sleeve strain are compared in Fig. 11. The measured sleeve strain at high temperature may include a slight aberration, but actual sleeve thrust is much less than that in the elastic theory.

After cracking of the specimen, circumferential reinforcement stress of C16 was twice as large as that of C22 in the pressure test because C16 was half the reinforcement ratio of C22. On the other hand, the reinforcement stress of H16 was at most 1.2 to 1.6 times higher than H22 because the sleeve thrust of H16 was reduced much more than that of H22 due to the differences in stiffness. Therefore, it is unnecessary to reinforce the concrete to the extent evaluated in the elastic theory.

3. Non-linear FE-analysis

Test results were simulated by non-linear FE-analysis. In addition, parametric studies by the same FEM were carried out to make sure of the general behaviour of the sleeve thrust. These analyses are discussed in this section.

3.1 Analytical Conditions: Fig. 12 shows the numerical model of the simulation analysis. Concrete body was modeled by eight node axisymmetric element with 3X3 Gaussian integration rule. Radial and circumferential reinforcements were modeled by line and point element, respectively. The model of parametric studies differed from Fig. 12 only in the outer diameter of concrete which was two times larger than Fig. 12. Cracking of concrete was judged by principal stress at each Gaussian point. After cracking has occurred the elastic modulus and Poisson's ratio in the direction perpendicular to the cracked plane were reduced to zero. Due to bond effects, concrete between cracks carries a certain amount of tensile force, so that gradual release of tensile force was assumed for concrete. The Drucker-Prager and von-Mises yield criterion were adopted for concrete and steel, respectively. Calculation was based on load incremental method and the convergence at each load step was achieved by the modified Newton-Raphson method. Fig. 13 shows stress-strain curves of concrete and steel. Material properties which were measured in the experiment were used in the simulation analysis. Those used in the parametric studies are listed in Table 3. Changes in material properties due to the rising temperature were assumed to be negligible, since the test period was very short and the temperature was considerably low.

Three analytical parameters were adopted in the parametric studies. They were reinforcement ratio, sleeve thickness and initial stress condition of concrete around a penetration. Taking the combinations of these parameters, eleven kinds of analyses, listed in Table 4, were carried out. Sleeve temperature was raised from 0°C to 100°C at 10°C intervals and temperature of surrounding concrete was assumed to be constant at 0°C in the all parametric studies.

3.2 Analytical Results

Simulation Analysis: Fig. 14 shows the pressure-deformation curves of the C22 specimen, and stress distributions of circumferential reinforcements are shown in Fig. 15. Analytical results were in agreement with test results, and it was clarified that the non-linear behaviour of reinforced concrete around a penetration can well be simulated by this FEM.

Parametric Study: Fig. 16 and Fig. 17 show the stresses of concrete and reinforcement in the circumferential direction. At the beginning, concrete was in elastic state, and radial cracks appeared at temperatures higher than 20°C. Then the concrete stress around the opening decreased. On the other hand reinforcement stress was the highest in the vicinity of the opening at every thermal loading step because concrete temperature was assumed to be constant at 0°C. The re-bar stress decreased to less than half at a distance of r=2a, where r is the radial distance from the center and a is the radius of the opening. So, thermal stress between r/a=1~2 is discussed herein. Thermal stress reduction factor β is defined by equation (2).

$$\beta = \frac{\int_a^{2a} \{(\sigma cn - \sigma co)\ Ac + (\sigma sn - \sigma so)\ As\}\ dr}{\int_a^{2a} (\sigma ce\ Ac + \sigma se\ As)\ dr} \qquad (2)$$

Where A is cross section area and suffix c, s, e, n, o indicate concrete, reinforcing bar, elastic analysis, non-linear analysis, and initial stress, respectively.

Fig. 18 shows the reduction factor β at 60°C, 80°C and 100°C. The thicker the sleeve or the lower the reinforcement ratio, the smaller β becomes. Particularly in the tensile state thermal stress is reduced to a great extent. For example, when initial tensile stress is 10 kgf/cm^2 and sleeve temperature is 60~100°C, the reduction ratio β is 0.36~0.53. Fig. 19 shows the thermal force by the elastic and non-linear analysis. It should be noted that the sleeve thrust is almost constant regardless of the sleeve thickness and that sleeve thrust gets larger with the increase of reinforcement ratio. Therefore, it is unnecessary to reinforce the concrete as much as evaluated in the elastic theory.

4. Conclusion

1) Sleeve thrust (i.e. compressive force in radial direction and tensile force in circumferential direction) actually reacts around a penetration by the thermal expansion of the penetration sleeve. It, however, decreases in accordance with the stiffness reduction by the cracking of concrete.
2) Circumferential tensile force by the sleeve thrust causes radial cracks around a pipe penetration. Crack widths are at a maximum in the early heating stage. Thereafter, the crack tends to close due to the thermal expansion of concrete.
3) In the early heating stage the reinforcement stress in circumferential direction becomes higher in accordance with the rising temperature. However, in the vicinity of a penetration it tends to decrease as heat is conducted to concrete.
4) Non-linear FE-analysis proved that sleeve thrust force is almost constant regardless of the sleeve thickness and it becomes larger with the increase of the reinforcement ratio. Therefore, it is unnecessary to reinforce the concrete as much as evaluated in the elastic theory.

Reference

[1] Timoshenko,S.P. and Goodier,J.N. Theory of elasticity, 3rd edition.

Table 1 Test parameters

Test type	Test specimen	Re-bar ratio: Circum-ferential direction	Re-bar ratio: Radial direction	Load: Sleeve temp.	Load: Inner pressure	Load: Outer pressure
Pressure test	C16	1.16% D16 @9cm	D16 22.5° spacing	-	0~100 kgf/cm²	0~15 kgf/cm²
	C22	2.11% D22 @9cm		-	0~100 kgf/cm²	0~15 kgf/cm²
Heating test	H16	1.16% D16 @9cm	D16 22.5° spacing	0~150 °C	-	0~15 kgf/cm²
	H22	2.11% D22 @9cm		0~150 °C	-	0~15 kgf/cm²

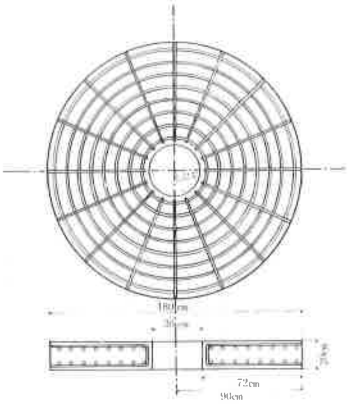

Fig.1 Test specimen

Table 2 Material properties

Concrete				Re-bar		Sleeve	
f_c kgf/cm²	f_t kgf/cm²	E $\times10^5$ kgf/cm²	α $\times10^{-5}$ /°C	f_y kgf/cm²	E $\times10^6$ kgf/cm²	E $\times10^6$ kgf/cm²	α $\times10^{-5}$ /°C
274	20.4	2.40	1.02	3713	2.09	2.09	1.06

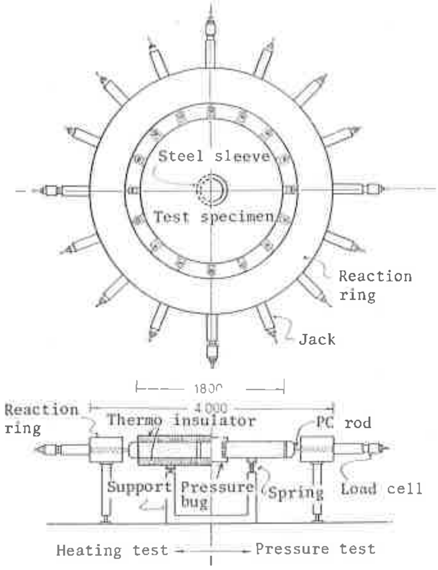

Fig.2 Test apparatus

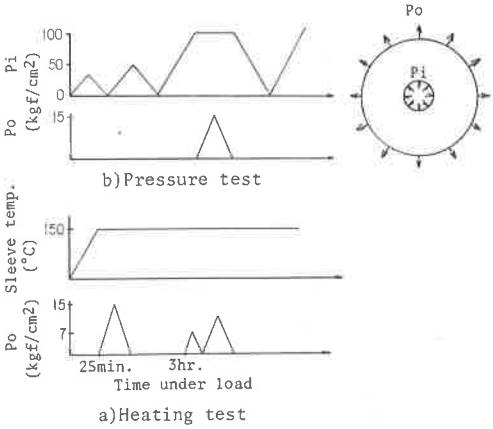

Fig.3 Loading histories

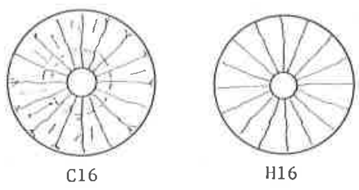

Fig.4 Cracking patterns of specimens

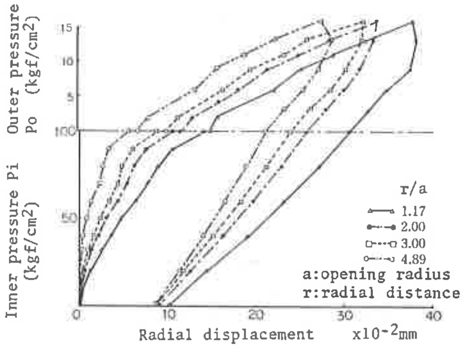

Fig.5 Pressure-deformation curves of C16

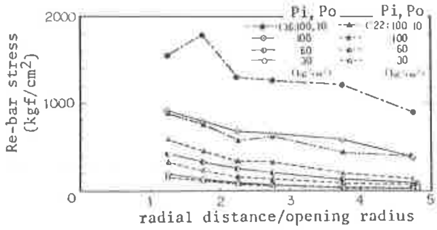

Fig.6 Stress distributions of the circumferential reinforcements (pressure test)

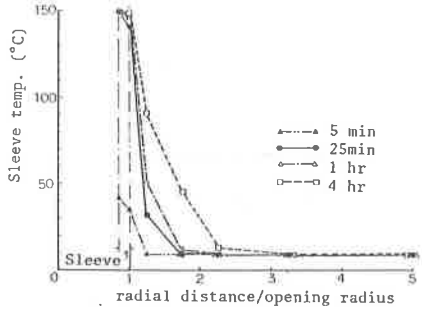

Fig.7 Temperature distributions of H16

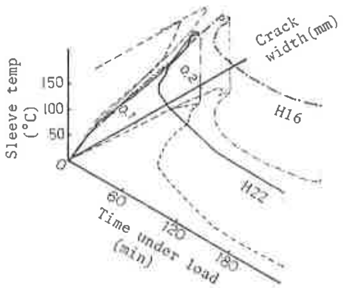

Fig.8 Relationships among cracking width, sleeve temperature and time under load

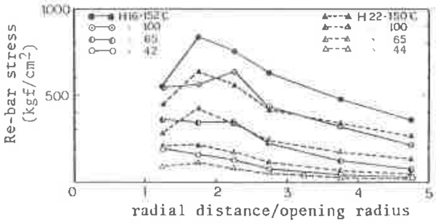

Fig.9 Stress distributions of the circumferential reinforcements (Heating test)

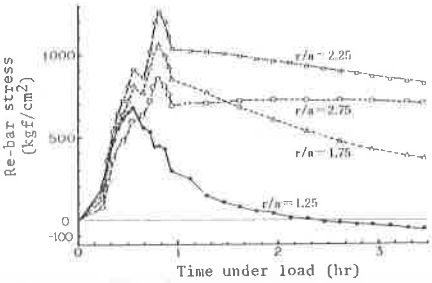

Fig.10 Relationships between stress of circumferential reinforcements and time under load (H16)

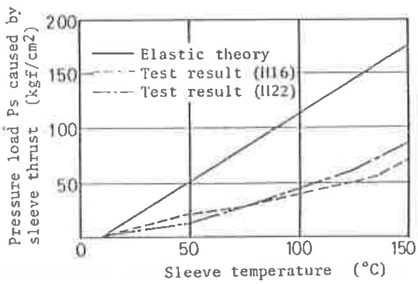

Fig.11 Pressure load Ps caused by sleeve thrust

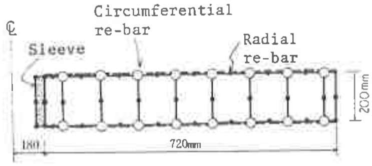

Fig.12 Numerical model of test specimen for FE-analysis

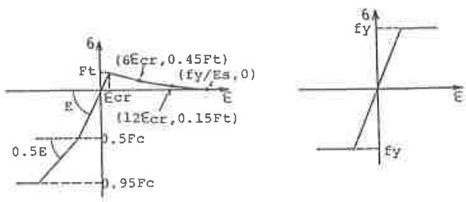

a) concrete

b) reinforcement and sleeve

Fig.13 Stress-strain curves of concrete and steel for FE-analysis

Table 3 Material properties adopted in parametric studies by FEM

Concrete				Steel		
f_c kgf/cm^2	f_t kgf/cm^2	E $\times10^5$ kgf/cm^2	α $\times10^{-5}$ /°C	f_y kgf/cm^2	E $\times10^6$ kgf/cm^2	α $\times10^{-5}$ /°C
240	24	2.1	1.0	3500	2.2	1.0

Table 4 Parameters of FE-analysis

No.	Sleeve thickness cm 2	4	6	8	Re-bar ratio % 1	2	3	4	5	Initial stress*1 kgf/cm^2 -20	10	20
1		○					○					
2	○						○					
3			○				○					
4				○			○					
5		○			○							
6		○				○						
7		○						○				
8		○							○			
9		○					○			○		
10		○					○				○	
11		○					○					○

*1 concrete stress in circumferential direction at the edge of the penetration

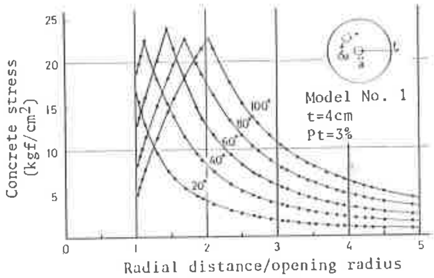

Fig.16 Concrete stress in circumferential direction by FE-analysis

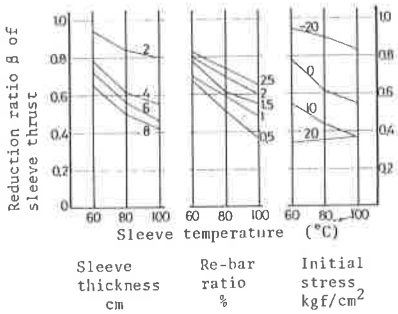

Fig.18 Reduction ratio β of sleeve thrust

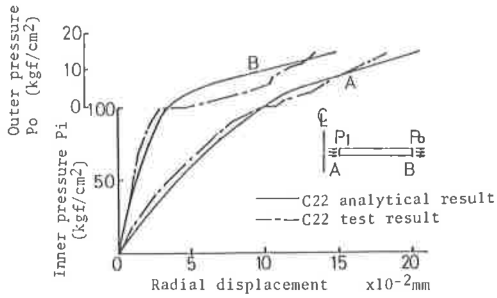

Fig.14 Pressure-deformation curve by simulation analysis (C22)

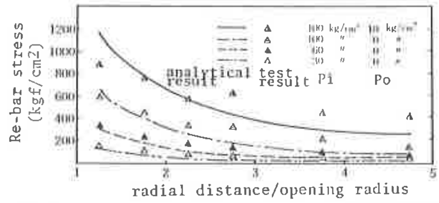

Fig.15 Reinforcement stress in circumferential direction by simulation analysis (C22)

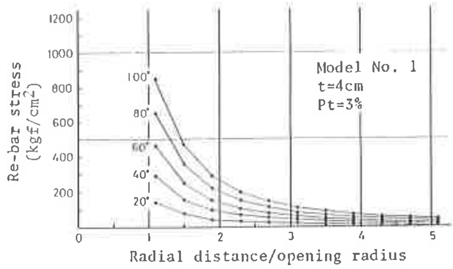

Fig.17 Reinforcement stress in circumferential direction by FE-analysis

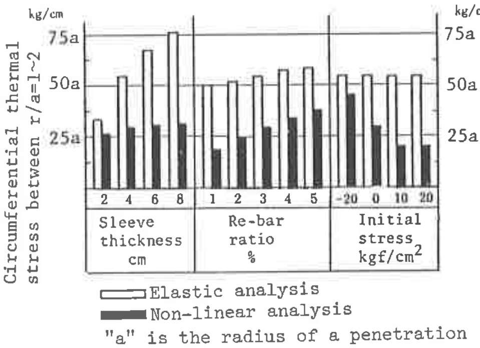

Fig.19 Comparison of sleeve thrust forces calculated by elastic and non-linear analysis (r/a=1~2,T=100 °C)